Meysam RADMEHR, Masoud RADMEHR, Salman AMIRKHAN

Aliabad Katoul Branch, Islamic Azad University

Kalman Filter Based Controller Design for Wind Energy Conversion

Abstract. *The active and reactive powers in the doubly-fed induction generator (DFIG) create a cross-coupling impact and inter-dependent relationship, affecting each other. This effect would not result in desirable reference tracking. To remove the cross-coupling impact, common decoupling methods such as state feedback decoupling can be applied. However, system robustness is too low against wind speed variation and consequently to that of rotor speed, which is inevitable. This disadvantage can be overcome by the suggestion of a Linear Quadratic Gaussian (LQG) controller. Using this controller, system robustness is improved versus both wind speed and DFIG parameters variation.*

Streszczenie. *W artykule opisano metodę odsprzężenia mocy czynnej w sterowaniu maszyną o dwustronnym zasilaniu (DFIG) poprzez zastosowanie regulatora LQG (ang. Linear Quadratic Gaussian). W ten sposób uzyskuje się poprawę dynamiki odpowiedzi algorytmu z odprzężeniem na zmianę prędkości wirnika oraz parametrów maszyny (**Regulator z filtrem Kalmana w sterowaniu przetwarzaniem energii wiatru**).*

Keywords: Doubly fed induction generator (DFIG), Active and reactive power, measurement noise, LQG controller.
Słowa kluczowe: generator asynchroniczny o dwustronnym zasilaniu (DFIG), moc czynna i bierna, szum pomiarowy, regulator LQG.

Introduction

Squirrel-cage induction machine, used in several wind-energy conversion systems, is mainly characterized by low cost, robustness and simplicity when directly connecting to the system [1]. However, wind-turbine should be designed in such a way to maintain the machine speed whatever the synchronous speed. This constraint reduces the possibility to increase the electrical energy produced for high wind speeds. This reduction can be defeat by the placement of a converter between stator and grid but it should be crossed by the full power of grid and must be correctly cooled. The application of a DFIG with low robustness against parameter variation and much more cost compared to Squirrel-cage induction generator, allows using a converter between rotor and stator which is designed only for a part of the full power of the machine (about 30%) [2]. By controlling correctly this convertor, variable-speed operation is allowed and electrical power can be produced from the stator to the grid and also from the rotor to the grid.

Many previous researches have been presented with different control schemes, considerably based on vector control concept (with stator flux or voltage orientation) with classical PI controllers as proposed by Pena in [1] and Poller in [3]. The same classical controllers are also used in the doubly-fed induction generator when grid faults appear like unbalanced voltages [4] and voltage dips [5]. Also, flicker problem could be solved with appropriate control strategies [6, 7]. A lot of these studies confirm that the reactive power control of stator can be an adapted solution to these different problems.

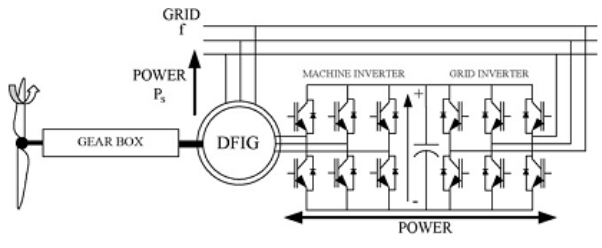

Fig.1. Doubly-fed induction generator connected to the gird

Active and reactive power controls are employed to adjust wind speed in an energy conversion system and to achieve a constant power coefficient between stator and grid, respectively. The active and reactive powers in the DFIG represent an interaction effect and inter-dependent relationship. Hence, the only use of classical PI controllers might not be successful. The solution is to apply the method of state feedback decoupling. The mentioned method is sensitive to parameter and wind speed variations. A control method, state observer-based controller, was used to employ as the second solution. Besides, there would be a problem in designing the observer if processing information occurs with noise. To defeat this difficulty, the application of LQG controller has been suggested in this paper. The performance of the DFIG is simulated and compared to that of PI controller with state feedback decoupling.

Wind turbine model

The power of the wind is proportional to the cube of its speed according to (1) [2].

$$P_M = \frac{1}{2}\rho\pi\lambda R^2 V_W^3 \tag{1}$$

However, only a part of this power can be converted into mechanical power.

$$P_M = \frac{1}{2}C_P\rho\lambda R^2 V_W^3 \tag{2}$$

c_p is a dimensionless number which is called a power coefficient. It depends on the wind turbine mechanical characteristics and is a function of the relative speed λ which represents the ratio of blade tip speed to wind speed.

$$\lambda = \frac{\Omega_1 R}{V_W} \tag{3}$$

Fig.2 shows an example of a typical curve $c_p(\lambda)$.The maximum value of the power coefficient c_p is reached for one particular value of the relative speed λ. This maximum value cannot be greater than 0.59 which represent the Betz limit.

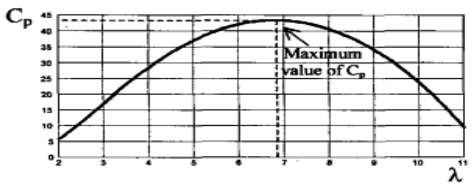

Fig.2. Example of $c_p(\lambda)$curve [2]

Knowing this curve and (2), it is possible to build some curves which gives the mechanical power versus the

rotating speed of the generator with the wind speed as parameter (Fig.3). Fixed speed operation appears in dashed lines and variable speed operation in full line.

We can note that the wind-turbine efficiency is much better for variable-speed operations than for fixed speed. The squirrel-age induction machine directly connected to the grid runs round the synchronous speed whatever the wind speed. This is carried out using a pitch adjustment of the turbine's blades. By allowing variable speed operations, the use of the DFIG makes it possible to consider a simplification of the pitch adjustment device and an improvement of the turbine's total efficiency.

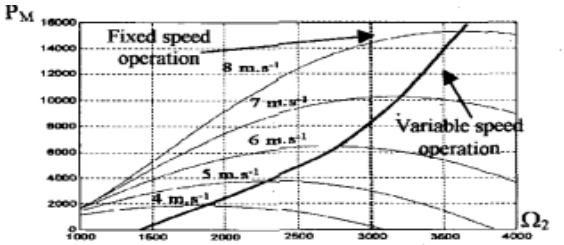

Fig.3. An Mechanical power versus rotating speed for several wind speeds [2]

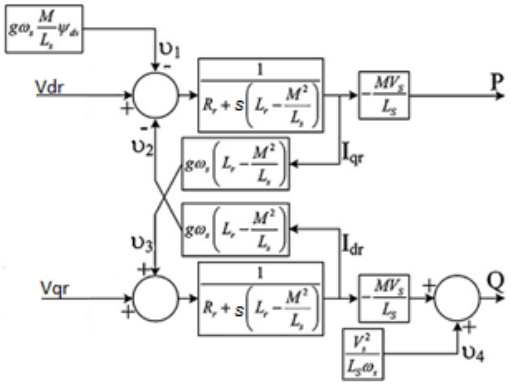

Fig.4. Block diagram of system

DFIG model

To achieve a stator active and reactive powers vector control we choose a d-q reference-frame synchronized with the stator flux. By setting the stator flux vector aligned with d-axis, we have [8]:

(4) $$\psi_{ds}=\psi_s,\psi_{qs}=0$$

(5) $$\Gamma_e=-p\frac{M}{L_s}I_{qr}\psi_{ds}$$

The electromagnetic torque and then the active power will only depend on the q-axis rotor current. Neglecting the per phase stator resistance R_s (that's the case for medium power machines used in wind energy conversion systems), the stator voltages and fluxes can be rewritten as follows:

(6) $$\begin{cases} V_{ds}=0; V_{qs}=V_s=\omega_s\psi_{ds} \\ \psi_{ds}=\psi_s=L_sI_{ds}+MI_{dr}; \psi_{dr}=L_rI_{dr}+MI_{ds} \\ \psi_{qs}=0=L_sI_{qs}+MI_{qr}; \psi_{qr}=L_rI_{qr}+MI_{qs} \end{cases}$$

The stator active and reactive power, the rotor fluxes and voltages can be written versus rotor currents as:

(7) $$\begin{cases} P=-V_s\frac{M}{L_s}I_{qr} \\ Q=\frac{V_s\psi_s}{L_s}-\frac{MV_s}{L_s}I_{qr} \end{cases}; \begin{cases} \psi_{dr}=\left(L_r-\frac{M^2}{L_s}\right)I_{dr}+\frac{MV_s}{\omega_sL_s} \\ \psi_{qr}=\left(L_r-\frac{M^2}{L_s}\right)I_{qr} \end{cases}$$

(8) $$\begin{cases} V_{dr}=R_rI_{dr}+\left(L_r-\frac{M^2}{L_s}\right)\frac{dI_{dr}}{dt}-g\omega_s\left(L_r-\frac{M^2}{L_s}\right)I_{qr} \\ V_{qr}=R_rI_{qr}+\left(L_r-\frac{M^2}{L_s}\right)\frac{dI_{qr}}{dt}+g\omega_s\left(L_r-\frac{M^2}{L_s}\right)I_{dr}+g\frac{MV_s}{L_s} \end{cases}$$

In steady state, the second derivative terms in (8) are nil .The third terms constitutes cross-coupling terms. The block- diagram representing the internal model of the system is presented in Fig. (4). Knowing (7) and (8), it is then possible to synthesize the regulators.

Rearrange (8) to (9):

(9) $$\frac{d}{dt}\begin{bmatrix} I_{dr} \\ I_{qr} \end{bmatrix}=\begin{bmatrix} -\frac{R_r}{\left(L_r-\frac{M^2}{L_s}\right)} & g\omega_s \\ -g\omega_s & -\frac{R_r}{\left(L_r-\frac{M^2}{L_s}\right)} \end{bmatrix}\begin{bmatrix} I_{dr} \\ I_{qr} \end{bmatrix}+ \begin{bmatrix} \frac{1}{\left(L_r-\frac{M^2}{L_s}\right)} & 0 \\ 0 & \frac{1}{\left(L_r-\frac{M^2}{L_s}\right)} \end{bmatrix}\begin{bmatrix} V_{dr} \\ V_{qr}-g\frac{M}{L}V_s \end{bmatrix}$$

Using the identification method of state space and (9), we have:

(10) $$A=\begin{bmatrix} -\frac{R_r}{\left(L_r-\frac{M^2}{L_s}\right)} & g\omega_s \\ -g\omega_s & \frac{R_r}{\left(L_r-\frac{M^2}{L_s}\right)} \end{bmatrix}$$

$$B=\frac{1}{\left(L_r-\frac{M^2}{L_s}\right)}\begin{bmatrix} 1 & 0 \\ 0 & 1 \end{bmatrix}\quad;\quad C=\begin{bmatrix} 1 & 0 \\ 0 & 1 \end{bmatrix}$$

where state, input and output variables are $\begin{bmatrix} I_{dr} & I_{qr} \end{bmatrix}^T$, $\begin{bmatrix} V_{dr} & V_{qr}-g\frac{M}{L_s}V_s \end{bmatrix}^T$ and $\begin{bmatrix} I_{dr} & I_{qr} \end{bmatrix}$ respectively.

LQG controller synthesis

In this section, the design of DFIG controller is discussed while assuming the processing information occurs with noise. LQG (Linear Quadratic Gaussian) controller is composed of an optimal regulator and an optimal observer (Kalman filter).Coefficient of the optimal regulator is obtained by resolving a Riccati equation. In order to design the observer, as understood, keeping nil speed of the observation error depends on the selected observer. The observer matrix L should be selected in a way that the observer pole placement is adjusted as far as on the left-side of the jω-axis. The fast keeping nil of the observer error is with magnified observer matrix, making the observer more sensitive to the observation noises (input noise and measurement noise). In fact, optimal-state observer (Kalman filter) is an optimal compromise between keeping nil speed of the observation error and the influences of noise processing [9].

Now, we describe details the design of LQG controller for the active power i.e. q-axis. Fig.7 shows a block diagram of the q-axis of the system controlled by an LQG controller. The control problem is described by the way of four vectors: y: measurements, e: error output to be regulated, u: control input, w: exogenous input (disturbances and references).

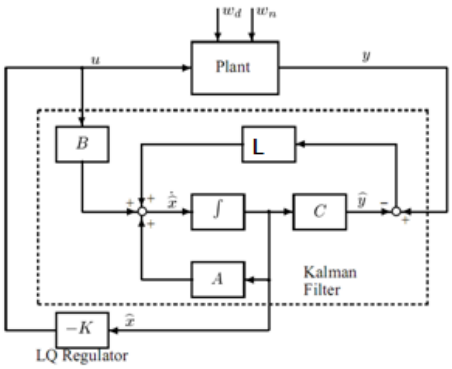

Fig.5. General Scheme of LQG controller and noisy system

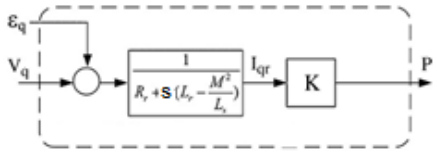

Fig.6. Simplified q-axis

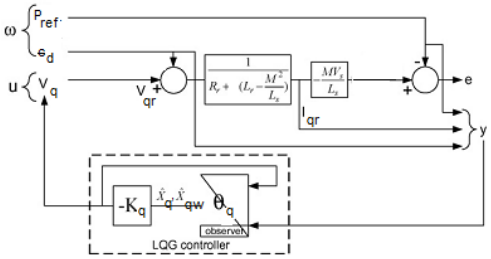

Fig.7. Block diagram of q-axis system with LQG controller

The aim is to find an observer-based controller allowing us to derive the control needed (u) to keep nil all control errors (e) from the measurements (y) whatever are the exogenous inputs (w). All exogenous signals (ε_q, P_{ref}) are considered constant. The LQG controller synthesis is presented bellow only for the q-axis because the methodology for the d-axis is similar.

The first step in the synthesis of the observer is to write the system as a standard problem.

$$
\begin{cases}
\dot{P}_{ref} = 0 \\
\dot{\varepsilon}_q = 0 \\
\begin{cases} X_{1q} = I_{qr},\ X_{2q}^T = \begin{pmatrix} P_{ref} & \varepsilon_q \end{pmatrix},\ u_q = V_{qr} \\ e = P - P_{ref},\ y^T = \begin{pmatrix} I_{qr} & P_{ref} & \varepsilon_q \end{pmatrix} \end{cases} \\
\begin{pmatrix} \dot{X}_{1q} \\ \dot{X}_{2q} \end{pmatrix} = \overbrace{\begin{pmatrix} A_{1\,1q} & A_{12q} \\ 0_{2\times 1} & A_{22q} \end{pmatrix}}^{A_q} \begin{pmatrix} X_{1q} \\ X_{2q} \end{pmatrix} + \overbrace{\begin{pmatrix} B_{1q} \\ 0 \end{pmatrix}}^{B_q} u_q + B_{\alpha q}\alpha_q \\
e = \overbrace{\begin{pmatrix} C_{e1q} & C_{e2q} \end{pmatrix}}^{C_{eq}} \begin{pmatrix} X_{1q} \\ X_{2q} \end{pmatrix} \\
y = \overbrace{\begin{pmatrix} C_{y1q} & C_{y2q} \end{pmatrix}}^{C_{yq}} \begin{pmatrix} X_{1q} \\ X_{2q} \end{pmatrix} + D_{\beta q}\beta_q
\end{cases}
\tag{11}
$$

The different matrices used in (11) are detailed in Appendix (2). The terms α and β (respectively state noise and measurements noise) are taken into account only for the synthesis of the observer (in our case, a Kalman filter).

The second step consists in determining an asymptotical control that must be applied to the system in steady state to ensure reference tracking and disturbance rejections. This control is obtained by resolving (12).This equation gives the two parameters T_{aq} (asymptotical trajectory) and G_{aq} (asymptotical gain).

$$
\begin{cases} A_{1\,1q} T_{aq} + B_{1q} G_{aq} = A_{12q} \\ C_{e2q} = C_{e1q} T_{aq} \end{cases}
\tag{12}
$$

By changing variable (13), the system is reduced to its controllable part (14):

$$
\xi_q = I_{qr} + T_{aq} X_{2q}
\tag{13}
$$

$$
\begin{cases} \dot{\xi}_q = A_{1\,1q}\xi_q + B_{1q}\tilde{u}_q \\ e = C_{e1q}\xi_q \end{cases}
\tag{14}
$$

$$
\tilde{u}_q = u_q - u_{aq} \qquad u_{aq} = -G_{aq} X_{2q}
$$

The feedback K_{1q} coefficient is calculated in such a way to minimize the following second order scale.

$$
J = \int_0^\infty (\xi_q^T Q_{cq} \xi_q + u_q^T R_{cq} u_q)\, dt
\tag{15}
$$

where ξ_q is the vector regulation error; u is the control input vector. R_{cq} and Q_{cq} are weighting matrices which Riccati equation ((17)) is produced by their regulation to (16).

$$
R_{cq} = 1 \quad , Q_{cq} = 100
\tag{16}
$$

$$
\begin{aligned}
&\exists P = P^T \geq 0 \\
&A_{1\,1q}^T P + P A_{1\,1q} + Q_{cq} - P B_{1q} R_{cq}^{-1} B_{1q}^T P = 0
\end{aligned}
\tag{17}
$$

After resolving the Riccati equation, and the resulting P matrix, the gain K_{1q} is given by:

$$
K_{1q} = R_{cq}^{-1} B_{1q}^T P
\tag{18}
$$

Considering (14), the control input can be described as:

$$
u_q = -\begin{pmatrix} K_{1q} & K_{1q} T_{aq} + G_{aq} \end{pmatrix} \begin{pmatrix} X_{1q} \\ X_{2q} \end{pmatrix}
\tag{19}
$$

The observer is designed to insure the minimum of variance for the estimation error in respect to the state and measurement noise variances (α, β). This observer is called as Kalman filter [10].

The observer structure is given below:

$$
\begin{cases} \dot{\hat{X}}_q = \begin{pmatrix} A_{1\,1q} & A_{12q} \\ 0 & A_{1\,1q} \end{pmatrix} \hat{X}_q + \begin{pmatrix} B_{1q} \\ 0 \end{pmatrix} u_q + L_q (y_q - \hat{y}_q) \\ \hat{y}_q = C_{yq} \hat{X}_q \end{cases}
\tag{20}
$$

Assuming $E\{\alpha_q \alpha_q^T\} = \alpha \geq 0; E\{\beta_q \beta_q^T\} = \beta \geq 0; E\{\alpha_q \beta_q^T\} = 0$, with Riccati equation, we have:

$$
\begin{aligned}
&\exists \gamma = \gamma^T \geq 0 \\
&\gamma A^T + A\gamma - \gamma C^T \beta^{-1} C\gamma + \alpha = 0
\end{aligned}
\tag{21}
$$

After resolving the Riccati equation ((21)), the gain L_q is given by (22).

(22) $$L_q = \gamma C^T \beta^{-1}$$

Finally, the q-axis controller is given by (23).

(23) $$\begin{cases} \dot{\hat{X}}_q = \begin{pmatrix} A_{1q} & A_{12q} \\ 0 & A_{1q} \end{pmatrix} \hat{X}_q + \begin{pmatrix} B_{1q} \\ 0 \end{pmatrix} u_q + L_q (y_q - \hat{y}_q) \\ \hat{y}_q = C_{yq} \hat{X}_q \\ u_q = -(K_{1q} \quad K_{1q} T_{aq} + G_{aq}) \begin{pmatrix} \hat{X}_{1q} \\ \hat{X}_{1q} \end{pmatrix} \end{cases}$$

The same methodology is used for the synthesis of the d-axis controller:

(24) $$\begin{cases} \dot{\hat{X}}_q = \begin{pmatrix} A_{1d} & A_{12d} \\ 0 & A_{1d} \end{pmatrix} \hat{X}_q + \begin{pmatrix} B_{1d} \\ 0 \end{pmatrix} u_d + L_d (y_d - \hat{y}_d) \\ \hat{y}_d = C_{yd} \hat{X}_d \\ u_q = -(K_{1d} \quad K_{1d} T_{ad} + G_{ad}) \begin{pmatrix} X_{1d} \\ X_{1d} \end{pmatrix} \end{cases}$$

where:

(25) $$\begin{cases} X_{1d} = I_{dr}, X_{2d}^T = (Q_{ref} \; v_3 \; v_4), u_d = V_{dr} \\ e = Q - Q_{ref}, y^T = (I_{dr} \; Q_{ref} \; v_3 \; v_4) \end{cases}$$

(26) $$\begin{cases} A_{1 1d} \quad T_{ad} + B_{1d} \, G_{ad} = A_{12d} \\ C_{e2d} = C_{e1d} \, T_{ad} \end{cases}$$

The different matrices mentioned in (24) are detailed in Appendix (2).

Simulation results

This section deals with the simulation of a 600kw generator connecting to a 220v/50Hz grid has been investigated. Generator parameters are presented in Table 1.

the tables is the width of the column – 8cm. An example of a table is presented below.

Table 1. DFIG parameters

Parameter	value
R_r	0. 62 Ω
R_s	0.455 Ω
L_s	0.006 Ω
L_r	0.003 Ω
M	0.078 Ω
J	0.5kg.m^2
f	0.0035N. m.s^{-1}

Reference Tracking

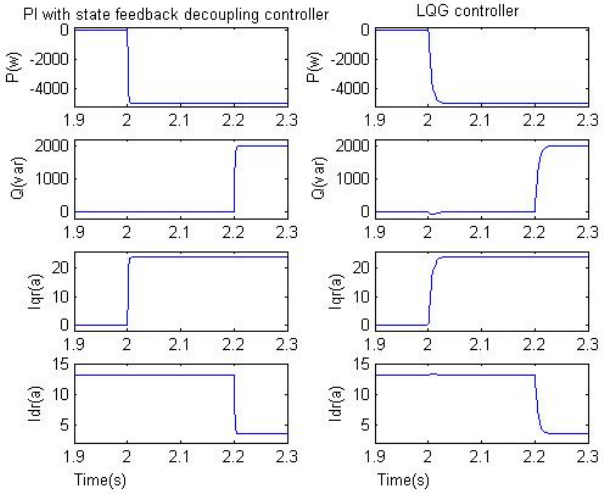

Fig.8. Reference tracking

To simulate the results of the active and reactive power reference tracking, ΔP = 5 kW and ΔQ = 2 kVarwere applied (respectively at t = 2 and t = 2.2) to the DFIG and then compared with LQG controller and PI controller with state feedback decoupling [11]. As shown in Fig. 8, independent reference tracking for both the active and reactive powers is performed properly in LQG and PI with state feedback decoupling controllers.

Effect of speed variation

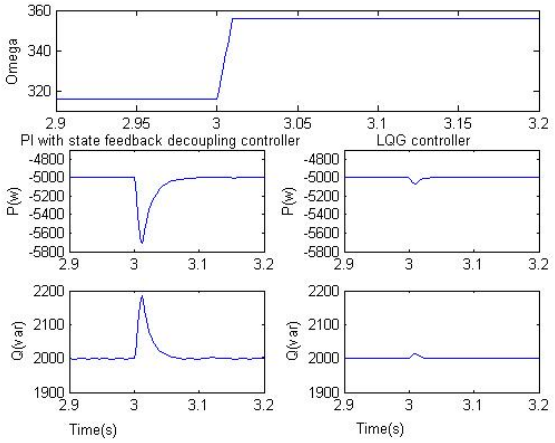

Fig.9. Effect of wind speed variation

To test the influence of wind speed variation on the controllers' performances, it was assumed that the rotor speed varies from 316 to 356 at t = 3. As indicated in Fig.9, LQG controller is robust to speed variation. Since PI controller with state feedback decoupling depends only on the generator parameters and dose not include perturbations, it is much more sensible to speed variation compared to the DFIG.

Effect of generator's parameter variation

The aim of this test is to analyze the influence of the DFIG parameters variations. The machine's model parameters have been deliberately modified with excessive variations: the values of the stator and the rotor resistances R_s and R_r are doubled and the values of the inductances L_s, L_r and M are divided by 2. ΔP = 5 kW at t = 2 and ΔQ = 2 kVar at t = 2.2 are applied to the DFIG and at $t = 2.8$, rotor speed is increased from 316 to 356 . These results show that parameters variation of the DFIG increases the time-response of the PI controller with state feedback decoupling. In addition, LQG controller's performance is not affected by parameters variation.

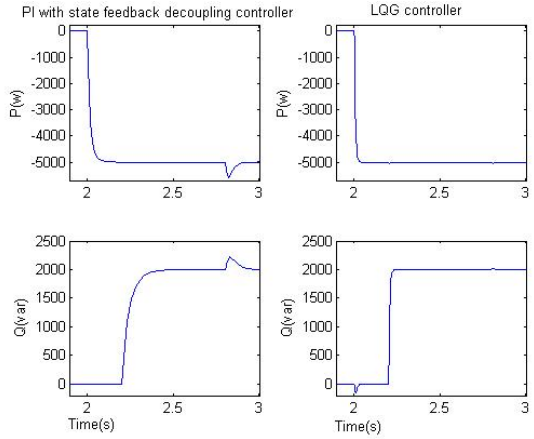

Fig.10. Effect of generator's parameter variation

Conclusion

As deduced from simulation results, using PI controller with state feedback decoupling can remove the interaction impact between d and q axis. However, the sensibility of the DFIG with PI controller with state feedback decoupling to parameters variation, especially speed, which is a common consequence, is indispensable. With the application LQG controller, the system can be robust against parameters variations and the interaction effect can be removed.

Appendix (1)

List of symbols:

$V_{ds}, V_{qs}, V_{dr}, V_{ds}$	Stator and rotor d-q voltages
$I_{ds}, I_{qs}, I_{dr}, I_{ds}$	Stator and rotor d-q currents
R_s, R_r	Stator and rotor per phase resistance
$\psi_{ds}, \psi_{qs}, \psi_{dr}, \psi_{ds}$	Stator and rotor d-q fluxes
L_s, L_r	Cyclic stator and rotor inductances
M	Magnetizing inductance
s	Laplace variable
p	Number of poles pairs
g	Induction machine's slip
ω_s, ω_r	Stator and rotor angular velocities

Appendix (2)

Matrixes used in LQG standard problem:

$$= \begin{pmatrix} A_{11q} & A_{12q} \\ 0 & A_{22q} \end{pmatrix} = \begin{pmatrix} \frac{-R_r}{(L_r - \frac{M^2}{L_s})} & 0 & \frac{1}{(L_r - \frac{M^2}{L_s})} \\ 0 & 0 & 0 \\ 0 & 0 & 0 \end{pmatrix}$$

$$B_q = \begin{pmatrix} B_{1q} \\ 0 \end{pmatrix} = \begin{pmatrix} \frac{1}{(L_r - \frac{M^2}{L_s})} \\ 0 \\ 0 \end{pmatrix}, B_{\alpha q} = I_3$$

$$C_{yq} = \begin{pmatrix} C_{y1q} & C_{y2q} \end{pmatrix} = I_3 \, , D_{\beta q} = I_3$$

$$C_{eq} = \begin{pmatrix} C_{e1q} & C_{e2q} \end{pmatrix} = \begin{pmatrix} \frac{-MV_s}{L_S} & -1 & 0 \end{pmatrix}$$

$$A_d = \begin{pmatrix} A_{11d} & A_{12d} \\ 0 & A_{22d} \end{pmatrix} = \begin{pmatrix} \frac{-R_r}{(L_r - \frac{M^2}{L_s})} & 0 & \frac{1}{(L_r - \frac{M^2}{L_s})} & 0 \\ 0 & 0 & 0 & 0 \\ 0 & 0 & 0 & 0 \\ 0 & 0 & 0 & 0 \end{pmatrix}$$

$$B_d = \begin{pmatrix} B_{1,d} \\ 0 \end{pmatrix} = \begin{pmatrix} \frac{1}{(L_r - \frac{M^2}{L_s})} \\ 0 \\ 0 \\ 0 \end{pmatrix} \; 'B_{\alpha d} = I_4$$

$$C_{yd} = \begin{pmatrix} C_{y1d} & C_{y2d} \end{pmatrix} = I_4 \quad , D_{\beta d} = I_4$$

$$C_{e,d} = \begin{pmatrix} C_{e1d} & C_{e2d} \end{pmatrix} = \begin{pmatrix} \frac{-MV_s}{L_s} & -1 & 0 & 1 \end{pmatrix}$$

REFERENCES

[1] Pena R., Asher G.M., A doubly fed induction generator using back to back converters supplying an isolated load from a variable speed wind turbine, IEEE Proceeding on Electrical Power Applications, 143, (1996).

[2] Heier S.,grid integration of Wind Energy Conversion Systems,John Wiley & Sons Ltd, Engeland,(1998).

[3] Poller M.A., Doubly –fed induction machine models for stability assessment of wind farms, in: Power Tech Conference Proceeding, 2003,IEEE, Bologna,vol.3, (2003), 23-26.

[4] Brekkan T.K.A., Mohan N., control of doubly fed induction wind generator under unbalanced grid voltage conditions, IEEE transaction on energy Conversion 22 ,(Mar(1))(2007) 129-135.

[5] Lopez J., Sanchis P., Roboam X., Marroyo L., Dynamic behavior ot the doubly fed induction generator during three-phase voltage dips, IEEE transaction on energy Conversion 22,(Sep(3)) (2007),709-717.

[6] Sun T., Chen Z., Blaabjerg F.,Filcker study on variable speed wind turbines with doublyfed induction generator, IEEE transaction on energy Conversion 20,(Dec(4)) (2005),896-905.

[7] Piegari L., Rizzo R.,A control technique for doublyfed induction generators to solve filcker problems in wind power generation, in internatinol powerandenerjy conference ,Putrajaya, Malaysia, 28 and 29Nov 2006.19-23.

[8] .Hopfensperger B., Atkinson D.J., Lakin R.A., Stator-flux-oriented control of a doublyfed induction machine with and without position encoder, IEEE Proc-Electr,Power Appl., Vol.147 ,No.4, (2000) ,241-250

[9] Patel R.V., Munro N., Multivariable System Thory and Design, Pergmon Press,(1982).

[10] Skogestad S., Postlethwaite I., Multivariable feedback control analysis and design, JOHN WILEY&SONS, Second Edition, (2001).

***Authors**:*

1-Meysam Radmehr (Corresponding author), Department of Electrical Engineering, Aliabad Katoul Branch, Islamic Azad University, Aliabad Katoul, Iran. E-mail: meysamradmehr59@yahoo.com

2-Masoud Radmehr, Department of Electrical Engineering, Aliabad Katoul Branch, Islamic Azad University, Aliabad Katoul, Iran. E-mail: masoud_radmehr@yahoo.com

3-Salman Amirkhan, Department of Electrical Engineering, Aliabad Katoul Branch, Islamic Azad University, Aliabad Katoul, Iran. E-mail: Amirkhan@aliabadiau.ac.ir